Biomaterials 130 (2017) 76–89

Contents lists available at ScienceDirect

Biomaterials

journal homepage: www.elsevier.com/locate/biomaterials

Testicular organoid generation by a novel *in vitro* three-layer gradient system

João Pedro Alves-Lopes*, Olle Söder, Jan-Bernd Stukenborg

Department of Women's and Children's Health, NORDFERTIL Research Lab Stockholm, Pediatric Endocrinology Unit, Q2:08, Karolinska Institutet and Karolinska University Hospital, SE-17176 Stockholm, Sweden

ARTICLE INFO

Article history:
Received 17 February 2017
Received in revised form
18 March 2017
Accepted 20 March 2017
Available online 23 March 2017

Keywords:
Testicular organoid
3D culture
Sertoli cells
Germ cells
De novo morphogenesis
Seminiferous tubules-like structures

ABSTRACT

A system that models the testicular microenvironment and spermatogonial stem-cell (SSC) niche *in vitro* has not been produced yet. Here, we developed and characterized a novel three-dimensional multilayer model, the Three-Layer Gradient System (3-LGS), which permits the generation of rat testicular organoids with a functional blood-testis barrier (BTB) and germ cell establishment and proliferation. The model is unique as regards the formation of cellular organizations that more closely represent the *in vivo* germ-to-somatic cell associations *in vitro*. Moreover, we also verified the roles of retinoic acid (RA), IL-1α, TNFα and RA inhibitors in germ cell maintenance and BTB organization *in vitro*. Treatment with RA was beneficial for germ cell maintenance, while IL-1α and TNFα were observed to impair the formation of testicular organoids and germ cell maintenance. Taking in account our characterization and validation results, we propose the 3-LGS as a new platform to investigate the SSC niche *in vitro* and to search for novel unknown factors involved in germ cell proliferation and differentiation. Moreover, we suggest that this model can be used in other scientific fields to study organogenesis and development by the generation of organoids.

1. Introduction

The testis has two main roles in male organisms: production of gametes and synthesis of androgens. The seminiferous tubules are composed of an internal epithelium formed of Sertoli cells, needed for germ cell differentiation, and external layers of smooth muscle-like cells known as peritubular cells. A network of thigh junctions (composed by zonula occludens-1/tight junction protein 1 (Zo-1/TJP1) and occludin proteins) between adjacent Sertoli cells forms the blood-testis barrier (BTB) and compartmentalize the seminiferous tubules in basal (below the BTB) and adluminal compartment (above the BTB) [1,2]. Moreover, the seminiferous tubules are supported by the interstitial tissue, which supplies oxygen, nutrients and important paracrine and endocrine hormones [3].

An *in vitro* system to model the testicular microenvironment has been tried for the last few decades. One of the first approaches applied was germ cell culture or co-culture on a monolayer of feeder cells in a two-dimensional (2D) fashion using standard culture dishes [4,5]. Although germ cells were co-cultured in close contact with feeder cells, such as Sertoli cells, it seems that the three-dimensional (3D) organization present *in vivo* is essential for germ cell proliferation and differentiation *in vitro* [6]. These observations led researchers to explore 3D culture approaches in order to closely model the testicular microenvironment *in vitro*. The formation of *de novo* seminiferous tubule-like structures was demonstrated when pre-pubertal primary testicular cells from rats and piglets were cultured into a supportive matrix [7] and/or grafted under the skin of immunodeficient mice [8,9]. Other researchers obtained similar structures when pre-pubertal mouse testicular cells were allowed to form cellular pellets which were then cultured on top of agar blocks [10]. Furthermore, spermatogenesis was recapitulated *in vitro* when pre-pubertal mouse testicular cells were cultured into agar and for 31 days [11–13].

An alternative 3D approach is to culture small testicular tissue samples placed on top of an agar block [14–16]. The principle of this method was already described in the 20th century [17]. However, it was not until 2011 that Sato and colleagues for the first time reported the birth of healthy mice after intra-cytoplasmic sperm injection using *in vitro*-produced sperm [18]. Recently, this system has been used by our group to differentiate rat spermatogonia into round spermatids [15]. Although *in vitro* production of functional

* Corresponding author.
E-mail address: joao.lopes@ki.se (J.P. Alves-Lopes).

http://dx.doi.org/10.1016/j.biomaterials.2017.03.025

sperm has been achieved in mice, a lot of basic understanding regarding testicular physiology remains to be studied, namely aspects related with the regulation of the spermatogonial stem-cell (SSC) niche in rats and humans. Furthermore, none of the previous models give a completely controlled *in vitro* platform to follow and influence testicular development and spermatogenesis. Thus a model which permits replication of testicular organogenesis and functionality is importantly needed.

In this work we aimed to develop and characterize a system that allows the reorganization of dissociated rat testicular cells into organoids that more closely represent the *in vivo* germ-to-somatic cell associations *in vitro* (Fig. 1). The Three-Layer Gradient System (3-LGS) permits the generation of testicular organoids with a functional BTB and germ cell establishment and proliferation. This model represents a new platform to explore, exclusively *in vitro*, the role of novel factors as well as the importance of distinct somatic testicular cells in the SSC niche.

2. Material and methods

2.1. Animals

Testes from 5–8-, 20- and 60-day *post partum* (d*pp*) Sprague Dawley male rats were collected and enzymatically dissociated in order to obtain total testicular cell suspensions. Animals were delivered by Charles River (Sulzfeld, Germany). All the experimental procedures were carried out in agreement with ethics permit number 280/14 accorded by Karolinska Institutet Ethics Committee for Experimental Laboratory Animals.

2.2. Sequential digestion

Rat testes were sequentially digested in order to obtain total testicular cell suspensions. Briefly, per experiment, 8 testes from 5–8-d*pp* rats, 4 testes from 20-d*pp* rats and ¼ testes from 60-d*pp*

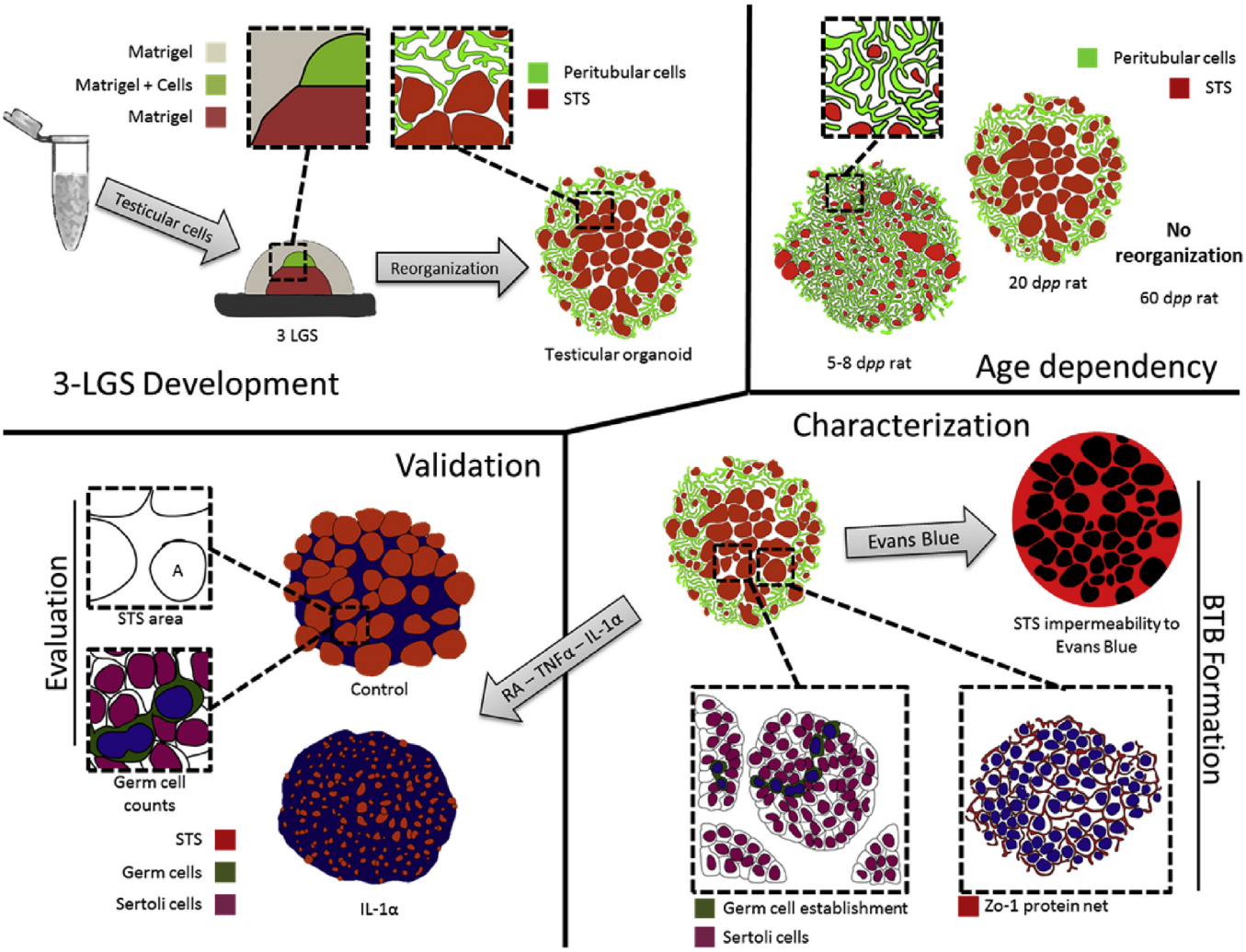

Fig. 1. Schematic overview of development, characterization and validation of the 3-LGS as a model to generate testicular organoids. During 3-LGS development, 20-day *post-partum* (20-d*pp*) rat testicular cells were combined with Matrigel and placed between two layers of that same material without cells. This arrangement led to cellular reorganization into spherical-tubular structures (STSs) and testicular organoid formation. Differences in colony organization were identified when testicular cells from different rat maturational stages were used to generate organoids. Characterization of 20-d*pp* rat testicular organoids showed that STSs are mainly formed of Sertoli cells and that germ cells can establish and proliferate on these structures. A functional blood-testis barrier was also displayed by STS impermeability to Evans Blue and detection of tight junction proteins. System validation was performed by verifying the roles of endogenous factors (RA, IL1-α and TNFα) and exogenous RA inhibitors (HX 531 and ER 50891) in germ cell maintenance and blood-testis barrier organization. These factors, with known effects *in vivo* on the testicular microenvironment, displayed similar influences on the 3-LGS organoids *in vitro*.

rats were decapsulated and mechanically disrupted using a needle and scalpel. In total, 3 experiments were performed per culture condition. Interstitial components were digested with collagenase 1A (P/N C2674, Sigma, St. Louis, USA) at 1 mg/mL in minimum essential medium alpha (MEM-α; P/N 22561-021, Gibco, CA, USA) supplemented with penicillin/streptomycin (1% pen/strep; P/N 15070-063, Gibco) for 10 min at 37 °C, shaking (120 rpm). Partially digested tissue was allowed to sediment for 10 min at 37 °C. Supernatant (interstitial fraction) was centrifuged at 300×*g* for 5 min and then re-suspended in MEM-α 1% pen/strep. The sediment, constituted mainly of seminiferous tubules, was further digested with collagenase 1A (1 mg/mL), DNAse 1 at 0.5 mg/mL (P/N 10104159001, Roche Diagnostics, Basel, Switzerland) and hyaluronidase at 0.5 mg/mL (P/N H3506, Sigma) for 15 min at 37 °C, shaking (120 rpm). Additional periods of 5 min digestion were performed in cases of incomplete results. The resulting cell suspension (tubular fraction) was centrifuged at 300×*g* for 5 min and then re-suspended in MEM-α 1% pen/strep. Interstitial and tubular fractions were combined and cellular concentration was determined.

2.3. Three dimensional co-culture

Hanging cell inserts (P/N PIHT12R48, Millipore, Billerica, MA, USA) were placed upside-down in an autoclaved plastic box. For a 3-LGS setting, 3 concentric drops of Corning® Matrigel® Growth Factor Reduced Basement Membrane Matrix, Phenol Red-Free (Matrigel; P/N 356231, Corning, Tewksbury, MA, USA) diluted 1:1 with MEM-α 1% pen/strep were sequentially applied to the bottom membrane surface of the insert. Firstly, a 5 μL drop was applied and the gelling process was accomplished after 15 min incubation at 37 °C. Secondly, a 3 μL drop with a final cellular concentration of 5.5, 11, 22, 44 or 88 million cells/mL, according to the experimental condition was placed on top of the previous drop. Gelling was allowed to occur for 15 min at 37 °C. Finally, an 8 μL drop was pipetted on top of the first two drops. The gelling process was concluded after 20 min at 37 °C. For the one-drop system setting, a 16 μL drop of Matrigel diluted 1:1 with MEM-α 1% pen/strep was applied, with a final cellular concentration of 5.5, 11, 22, 44 or 88 million cells/mL, according to the experimental condition. Gelling lasted 20 min at 37 °C. Matrigel was always handled on ice to avoid undesired gelling. Both three-layer gradient and one-drop culture systems were placed in 24-well plates (P/N 734-2325, VWR, Radnor, PA, USA) and 0.6 mL of culture medium was added per well.

2.4. Culture conditions

MEM-α 1% pen/strep supplemented with 10% KnockOut serum replacement (KSR; P/N 10828-028, Gibco) was used as basic culture medium. Supplementation with 10 nM–100 μM RA (P/N R2625, Sigma), 10^{-7} M melatonin (P/N M5250, Sigma), 10 nM–10 μM M RARα antagonist (ER 50891; P/N 3823, Tocris, Bristol, United Kingdom), 1 nM–1 μM M retinoid X receptor antagonist (HX 531; P/N 3912, Tocris), recombinant rat IL-1α at 1–10 ng/mL (P/N 500-RL-025, R&D Systems, Minneapolis, USA) and rat TNFα at 1–10 ng/mL (P/N T5944, Sigma) were used depending on the experimental context. 3D co-cultures were incubated at 35 °C, with 5% CO_2 and half medium volume (0.3 mL) was changed every second day.

2.5. Live imaging

3D co-cultures were visualized using a bright-field Eclipse TE 2000 microscope (Nikon, Tokyo, Japan) and pictured with an Infinity 1-2C digital camera (Lumenera, Ottawa, Canada) daily for 10 days and later every second day.

2.6. Migration assay

Relative migration area was determined for each different rat age (5–8-, 20- and 60-d*pp*), when total testicular cell suspensions were co-cultured using the 3-LGS with a final cellular concentration of 44 million cells/mL. Briefly, the area occupied by cells was measured from day 0 until day 7 by means of the image analysis program ImageJ (U. S. National Institutes of Health, Bethesda, USA). Relative migration area was calculated using the following equation:

$$\textit{Relative migration area} = \frac{\textit{colony area day } 0 - \textit{colony area day } x}{\textit{colony area day } 0} \times 100$$

where x represents the experimental day of analysis (0–7).

2.7. Whole-mount staining

Samples co-cultured in the 3-LGS were collected from the inserts using a scalpel. Seminiferous tubules from 5–8-, 20- and 60-d*pp* rats were mechanically separated to be used as positive and negative controls (Suppl. Fig. 1). After fixation in 4% paraformaldehyde (P/N 02176, HistoLab, Gothenburg, Sweden) for 2 h at 4 °C plus 30 min at room temperature (RT), antigen retrieval in 10 mM sodium citrate (P/N C7254, Sigma) aqueous solution, 0.05% Tween® 20 (P/N K38485272825, Merck, Frankfurt, Germany), pH 6 was applied for 15 min at 95 °C. The samples cooled down for 30 min and then were washed 3 times with phosphate-buffered saline (PBS; P/N 70013-016, Gibco). Permeabilization was performed by washing 3 times with PBS 1% Triton® X-100 (Triton; P/N 11869, Merck) for 30 min at RT. Blocking was achieved by incubating twice with PBS 1% Triton, 10% Normal Donkey Serum (DS; P/N 017-000-121, Jackson Immuno Research, West Grove, PA, USA), 0.2% sodium azide (P/N K21403688513, Merck), 1% affini pure fab fragment donkey anti-mouse IgG (frag; P/N 715-007-003, Jackson Immuno Research) for 1 h at RT. Primary antibodies were incubated against the protein of interest and at the desired dilution in PBS 1% Triton, 10% DS, 0.2% sodium azide (Table 1) for 3 days at 4 °C. Non-specific rabbit and mouse IgGs were used to create negative controls when incubated in place of primary antibodies (Table 1). Samples were then washed 3 times with PBS 1% Triton, 10% DS for 1 h at RT, followed by 3 washes with PBS 1% Triton for 10 min at RT and 3 washes with PBS 1% Triton, 10% DS, 0.2% sodium azide for 1 h at RT. Additional 3 washes with PBS 1% Triton for 10 min at RT were followed by secondary antibody incubation at the desired dilution in PBS 1% Triton, 10% DS, 0.2% sodium azide (Table 1) for 3 days at 4 °C. Counter-staining was performed by the addition of Pure Blu™ DAPI Nuclear Staining Dye (P/N 135-1303, BioRad Hercules, CA, USA) to the secondary antibody solution at the second day of incubation to obtain a final concentration of 4 μg/mL. Finally, the samples were washed 5 times with PBS 1% Triton for 15 min at RT and then mounted as described below. Stained samples were placed on 24 × 60 mm coverslips (P/N 10212460C, Citoglas, Nanjing, China) and surrounded by a ring of silicon grease (P/N 335148, VWR) moulded using a 3 mL syringe (P/N 613-2050, VWR). Next, a drop of 2% low-melting-point agarose (P/N 15517-022, Invitrogen, Carlsbad, CA, USA) was pipetted on top of the sample and left to solidify for 5 min at RT. PBS was added to cover the agarose-fixed sample until the formation of a convex meniscus. A coverslip (24 × 24 mm) was placed on top of the preparation and gently pressed down, expelling excess PBS. Both 2D and 3D pictures were obtained by using a Zeiss LSM 700 confocal microscope (Carl Zeiss, Oberkochen, Germany).

Table 1
Details of the antibodies utilized.

	Antibody	Concentration (mg/mL)	P/N	Company
α-Sm	Monoclonal Anti-a Smooth Muscle Actin	Ascites (1:500)	A 2547	Sigma
Sox9	Anti-Sox9 Polyclonal Antibody	0.00426	AB5535	Merck Millipore
Ddx4 - rabbit	Anti-DDX4/MVH antibody - Primordial Germ Cell Marker	0.01667	ab13840	Abcam, Cambridge, United Kingdom
Ddx4 - mouse	Anti-DDX4/MVH antibody [mAbcam27591]	0.01667	ab27591	Abcam
Vimentin	Anti-Vimentin (V9)	0.005	MMS-459S	Convance, Princeton, USA
Zo1	Rabbit anti-ZO-1	0.0025	61–7300	Invitrogene, Carlsbad, USA
Occludin	Anti-Occludin	0.0365	ab168957	Abcam
Plzf	PLZF Antibody (H-300)	0.008	sc-22839	Santa Cruz Biotechonology
Pcna	Anti-PCNA antibody [PC10]	0.0067	ab29	Abcam
IgGs ms	Normal mouse IgG	0.004	sc-2025	Santa Cruz Biotechonology
IgGs rb	Rabbit IgG, polyclonal	0.002	ab 27478	Abcam
Cy3	Donkey anti rabbit Cy™3- conjugated AffiniPure F(ab)2 Fragments	0.003	11483299	Thermo Fisher, Waltham, USA
Alexa 488	Donkey anti-mouse Alexa 488 IgG	0.003	715546150	Thermo Fisher

2.8. Immunofluorescence

Co-culture systems were fixed in 4% paraformaldehyde or in Bouin's solution (P/N HT10132, Sigma), for 2.5 h or overnight respectively, at 4 °C. After dehydration by using an ascending ethanol series plus butyl acetate (P/N 45860, Sigma) (70%, 80%, 96%, 99.6% ethanol and butyl acetate, in all cases overnight), samples were embedded in Paraplast X-TRA® (P/N P3808, Sigma) and kept overnight at 61 °C. Samples were cut at 5 μm at KI facilities. Sections were de-paraffinized and rehydrated using xylene and a descending ethanol series (2 × 10 min xylene, 10 min 99.6%, 5 min 99.6%, 5 min 96% and 5 min 70% ethanol). Antigen retrieval was carried out in 10 mM sodium citrate aqueous solution, 0.05% Tween® 20, pH 6, for 15 min at 95 °C. The samples were allowed to cool for 30 min and were then washed for 5 min in running water. Additional washing with Tris-Buffered Saline (TBS; P/N sc-24951, Santa Cruz, CA, USA) was carried out twice for 5 min, followed by a blocking step using TBS, 10% DS and 1.5% Bovine Serum Albumin (BSA; P/N 001-000-162, Jackson Immuno Research) for 30 min at RT. Primary antibodies were incubated at the desired dilution in TBS, 10% DS and 1.5% BSA (Table 1) overnight at 4 °C. The sections were washed in running water for 5 min and then twice in TBS for 5 min at RT. Secondary antibody incubation at the desired dilution in TBS, 10% DS, 1.5% BSA (Table 1) was carried out for 30 min at RT. Counter-staining was carried out by adding DAPI to the same solution, obtaining a final concentration of 4 μg/mL. Finally, the samples were washed twice in TBS for 5 min at RT and then mounted in VECTASHIELD HardSet Antifade Mounting Medium (P/N H-1400, Vector, CA, USA). Preparations were visualized using an Eclipse E8000 microscope (Nikon, Tokyo, Japan) and pictured with a 12.5 million-pixel cooled digital colour camera system (Olympus DP70, Tokyo, Japan).

2.9. Histochemistry

Periodic acid-Schiff staining was carried out by means of a commercially available kit (P/N 101646, Merck). Briefly, sections were de-paraffinized and rehydrated using xylene plus a descending ethanol series, followed by washing twice in distilled water for 5 min. Sections were treated with periodic acid for 5 min and then washed under running water for 3 min and in distilled water twice for 5 min. Samples were then exposed to Schiff's reagent for 15 min. Next, washing under running water for 3 min and twice in distilled water for 5 min was performed. Mayer's Hemalaun solution (P/N 1092491000, Merck) was applied for 1 min in order to stain nuclei. Sections were washed in running water for 3 min and then dehydrated by an ascending ethanol series plus xylene (5 min 70%, 5 min 96%, 5 min 99.6%, 5 min 99.6% ethanol, 2 × 10 min xylene). Pertex (P/N 00811, HistoLab) was applied to mount the slides. Preparations were visualized using an Eclipse E8000 microscope (Nikon) and pictured with a 12.5 million-pixel cooled digital colour camera system (Olympus DP70).

2.10. Counting

After whole-mount staining, samples were analysed by confocal microscopy. A Z-stack command was employed to generate a superficial 3D overview of the co-culture system. Briefly, pictures were produced every 3 μm from samples of approximately 50–100 μm thickness, depending on the co-culture system. Next, positive cells stained for a marker of interest as well as total cell numbers were counted. A ratio between the number of cells stained for a marker of interest and total cell counts was calculated, allowing comparison of different treatments.

2.11. Blood testis barrier functionality

Co-cultures were collected after 7 days of culture and washed 3 times with PBS. Incubation with 0.4% Evans Blue (P/N E2129, Sigma) in PBS for 30 min at 35 °C was then performed to evaluate BTB functionality. Samples were washed 3 times with PBS and finally mounted for whole-mount staining as described above. To further explore BTB formation *in vitro*, co-cultures were whole-mount stained against Zo-1 and occludin (two tight-junction markers), using primary antibodies at the desired dilution (Table 1). In order to assess live cellular organization, samples were incubated with 2% Evans Blue in PBS for 30 min at 35 °C. Co-cultures were then washed 3 times with PBS and finally mounted for whole-mount staining. Both 2D and 3D pictures were obtained by Zeiss LSM 700 confocal microscopy.

2.12. Statistical analysis

One-way ANOVA, and one-way repeated measures ANOVA were applied to perform statistical analysis, using SigmaPlot software ver. 12.0 (Systat Software Inc., IL, USA) as stated in the figure legends. Each experimental setup was repeated at least 3 times, and the means and standard deviations were used in statistical analysis and in the figures. The *P* value was considered significant if it was ≤ 0.05.

3. Results

3.1. The 3-LGS stimulates formation of seminiferous-like structures

Testicular cell suspensions from 20-day d*pp* rats reorganized into seminiferous-like structures when cultured into a layer of Matrigel placed between two cell-free layers of Matrigel (Figs. 1 and

2a). In contrast, cellular reorganization was not observed when only one layer of Matrigel was used (controls). In order to compare the two systems, we used the same cellular concentrations in the middle layer of the 3-LGS and in the one-layer condition. Additionally, the same final volume was used for both systems (Fig. 2a). Immunofluorescence staining for SRY (Sex-Determining Region Y)-Box 9 Protein (Sox9), Sertoli cell marker, and α-Sm, a peritubular cell marker, confirmed that the organization observed in the 3-LGS was not detected when only one layer was used (Fig. 2b).

3.2. Changes in cell maturation stage and concentration lead to differences in colony organization

In order to find the best cellular concentration to proceed, serial concentrations of 5.5, 11, 22, 44 and 88 million cells/mL were assayed (20-d*pp* rat cells; 3-LGS). Although all concentrations used resulted in the formation of sphere-tubular structures (STSs) (Suppl. Fig. 2a and b), we adopted 44 million cells/mL for future experiments because it was more practical for later evaluation

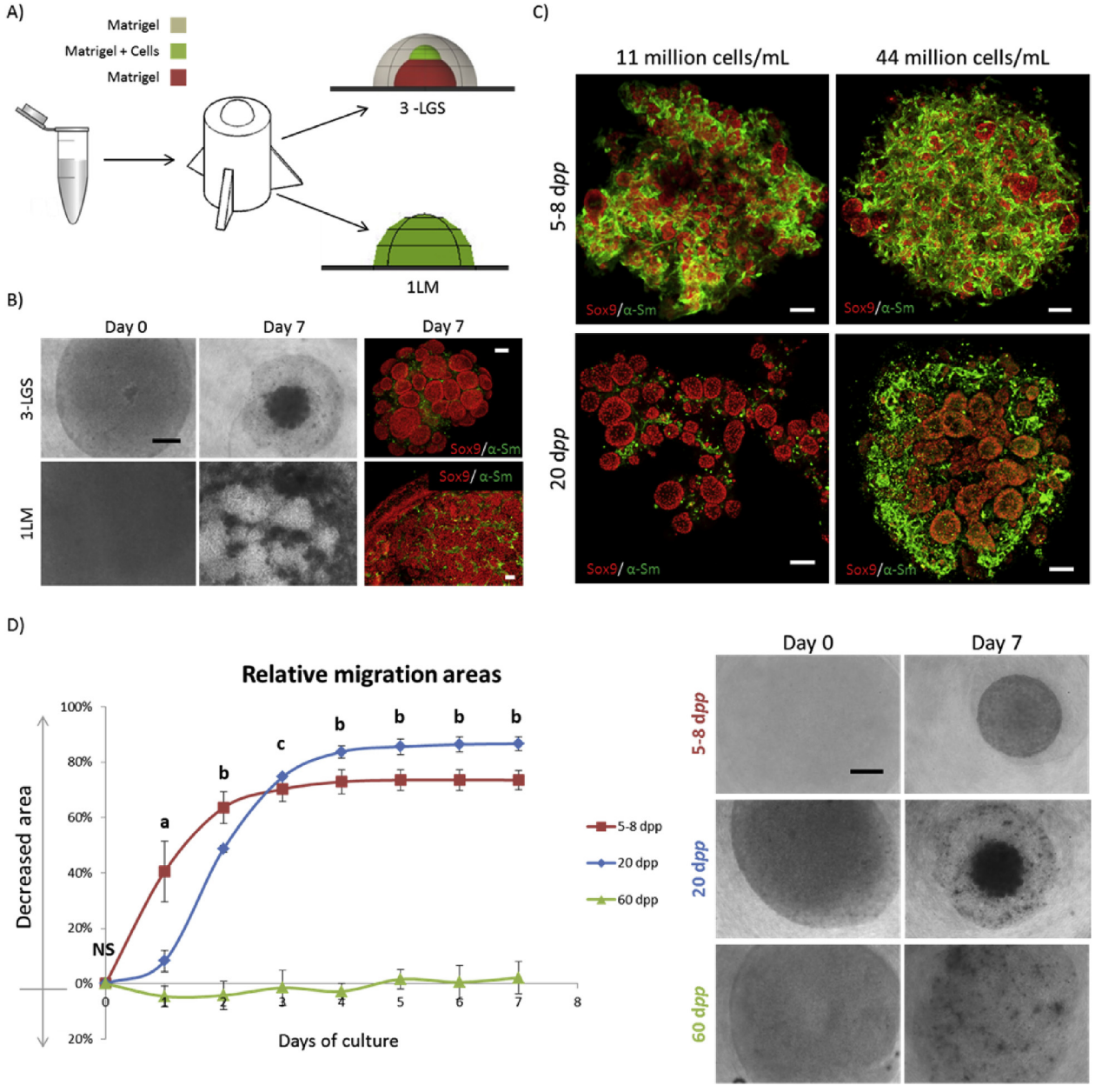

Fig. 2. Testicular organoid generation and cell maturational stage dependency. (A) Schematic view of the 3-LGS and one-layer Matrigel (1LM) model setup. (B) Differences in cellular reorganization, day 0 (bright field) and day 7 (bright field and immunofluorescence staining against Sox9 and α-Sm) when the 3-LGS and one-layer Matrigel setup were applied to culture 20-d*pp* rat testicular cells. (C) Colony organization of 5–8- and 20-d*pp* rat testicular cells cultured using the 3-LGS at low (11 million cells/mL) and high (44 million cells/mL) concentration displayed by immunofluorescence staining of Sox9 and α-Sm. (D) Relative migration areas of 5–8-, 20- and 60-d*pp* rat testicular cells cultured for 7 days using the 3-LGS. Bright-field pictures from days 0 and 7 showing different migration profiles depending on cellular maturational stage. Scale bars: B+C: 100 μm (immunofluorescence); B+D: 500 μm (bright field). Positive and negative controls for Sox9 and α-Sm are shown in Suppl. Fig. 1 Significance (methods: One Way ANOVA, normality test: Shapiro–Wilk; all pairwise multiple comparisons: Holm-Sidak): a = 5–8 d*pp* vs. 20 d*pp* and 5–8 d*pp* vs. 60 d*pp*: $P < 0.001$; b = 5–8 d*pp* vs. 20 d*pp*: $P < 0.01$, 20 d*pp* vs. 60 d*pp* and 5–8 d*pp* vs. 60 d*pp*: $P < 0.001$; c = 20 d*pp* vs. 60 d*pp* and 5–8 d*pp* vs. 60 d*pp*: $P < 0.001$; NS = no statistically significant differences between the groups.

steps. At this concentration, STSs were distributed in the centre of the colony and were connected, which facilitated further handling (Suppl. Fig. 2a and b). In parallel, similar cell concentrations were tested using the one-layer setup to further compare the morphogenic capacity of both systems. STS were always observed in the 3-LGS conditions but not in the one-layer setup at all concentrations tested (Suppl. Fig. 2a).

In order to detect differences in colony organization at different testicular maturational stages (5–8-, 20- and 60-d*pp* rats, covering pre-pubertal, pubertal and post-pubertal stages respectively), cells at serial concentrations of 5.5, 11, 22, 44 and 88 million cells/mL were cultured applying 3-LGS conditions (Suppl. Fig. 2c). As mentioned before, STSs were observed at all concentrations utilized from 20-d*pp* rats. Regarding 5–8-d*pp* rats, STSs were only formed when low cellular concentrations were applied (5.5, 11 or 22 million cells/mL). In contrast, STSs were not observed when high cellular concentrations (44 or 88 million cells/mL) were used. Testicular cell suspensions from 60-d*pp* rats were also cultured using the same approach, but no STS formation was detected at any concentration utilized (Suppl. Fig. 2c).

Differences in terms of cellular organization were further investigated by immunofluorescence staining for Sox9 and α-Sm. Low-concentration samples (11 million cells/mL) and high-concentration samples (44 million cells/mL) from 5–8- and 20-d*pp* rats cultured for 7 days were whole-mount stained and analysed by confocal microscopy (Fig. 2c). At both low and high concentrations, STSs were confirmed to be present in 20-d*pp* cultures. Peritubular cells were present around the STSs. In contrast, few STSs were present at low and even less at high cell concentrations from 5–8-d*pp* rats. In this case, peritubular cells were distributed throughout the colony and were observed to involve the formed STSs (Fig. 2c). Regarding 60-d*pp* rat testicular cells, a similar evaluation could not be performed due to technical limitations and a lack of STS formation.

The migration profiles of 5–8-, 20- and 60-d*pp* rat testicular cells were followed to further explore differences in organization at these different maturational stages. For this, 44 million cells/mL were cultured (3-LGS) and cellular migration followed for 7 days. 5–8-d*pp* rat testicular cells were observed to reduce by 40.5% of their initial occupied area in after 1 day in culture. This decreased area was superior to that of 20-d*pp* rat cells (8.2% decreased area) and 60-d*pp* cells (4.6% increased area) at the same experimental time point. On the second day of culture, 5–8-d*pp* rat testicular cells showed a 63.6% reduction in area, 20-d*pp* cells a 48.7% reduction and 60-d*pp* cells a 4.2% increase of the initial occupied area. Cellular migration was detected to decelerate at day 4, when 5–8-d*pp* rat cells showed a 72.9% reduction and 20-d*pp* cells an 83.7% reduction of the initial area. The colony areas remained constant up to the last day of the assay, with decreases of 73.6% for 5–8-d*pp* rat cells, 86.6% for 20-d*pp* cells and 2.1% for 60-d*pp* cells. Altogether, 5–8-d*pp* rat testicular cells were found to migrate faster but to form less compact STS colonies compared with 20-d*pp* cells, while 60-d*pp* rat testicular cells did not show active migration capacity or STS formation (Fig. 2d).

3.3. Self-reorganization in 3-LGS leads to BTB formation and Sertoli cell epithelization

Sertoli cells from 20-d*pp* rats demonstrated the ability to self-reorganize into STSs after 7 days of culture. The presence of other cell types was also identified between or on the surface of STSs by DAPI counterstaining (Suppl. Fig. 3a). This histological arrangement of Sertoli cells was shown by periodic acid-Schiff staining as well as immunofluorescence staining against Sox9 and α-Sm (Fig. 3a and b). Although 20-d*pp* rat Sertoli cells demonstrated an arrangement similar to that *in vivo*, peritubular cells did not completely involve STSs in the 3-LGS in the same extent as observed in seminiferous tubules *in vivo* (Fig. 3a and b). Instead, some α-Sm-positive cells were observed to be dotted around the STS-formed colony (Fig. 3a and b).

Impermeability of 0.4% Evans Blue dye (Fig. 3a) and the expression of Zo-1 and occludin tight junction proteins were also verified, displaying evidence of the presence of a functional BTB in STSs (Fig. 3b). Sertoli cell epithelization was also detected by means of 2% Evans Blue treatment. In this last experiment, STSs were disrupted by the high concentration of Evans Blue and the dye was allowed to surround cells from both inner and outer sides, enabling visualization of Sertoli cell columnar epithelialization (Suppl. Fig. 3b).

3.4. Germ cells can be maintained on the organoids

After the characterization of somatic cell organization, the potential of the 3-LGS to generate a testicular organoid *in vitro* was further explored by searching for the presence of germ cells (Ddx4-positive cells). These cells were identified on the STSs formed from 20-d*pp* rat cells cultured for up to 21 days (Figs. 3c and 4a and Suppl. Fig. 4b). Additionally, undifferentiated germ cells (Plzf-positive cells) were found to form cellular chains connected by cytoplasmic bridges (Fig. 3c and Suppl. Fig. 4a) lasting for 21 days in culture (Suppl. Fig. 4b). Moreover, undifferentiated germ cell proliferation (Plfz/Pcna double positive staining) was observed on the organoids 10 and 21 days after the beginning of the cultures (Fig. 3c). In addition to the Pcna staining, mitotic figures were also observed in germ cells in culture for 10 and 21 days (Suppl. Fig. 5a and b respectively), confirming the proliferation status of these cells.

3.5. Retinoic acid (RA) treatment showed a beneficial effect on germ cell maintenance

To investigate the role of RA in germ cell maintenance on the organoids, testicular cells (20-d*pp*) were cultured with RA, ER 50891 (RARα antagonist) and HX 531 (RXRs antagonist) for 10 days using the 3-LGS. Regarding RA treatment, the ratio germ cell count/total cell count was higher (12%) than in the controls (7.1%) when 1 μM was applied. At a higher molarity of RA (100 μM), this ratio was lower than in the controls (Fig. 4b).

Concerning the treatment with ER 50891, it was observed an inverse relationship between germ cell maintenance and the molarity of the inhibitor. The ratio germ cell count/total cell count was always observed to be lower than in control cultures (i.e. < 7.1%) and it decreased significantly from 6.2% to 2.0% when ER 50891 molarities of 10 nM and 10 μM were utilized, respectively (Fig. 4a and b). Regarding treatment with HX 531, all molarities used (ranging from 1 nM to 1 μM) showed no effect in terms of germ cell maintenance, and the germ cell count/total cell count ratios were, in all cases, similar to control values (Fig. 4b).

3.6. Interleukin 1 alpha (IL-1α) and tumor necrosis factor alpha (TNFα) impaired the formation of testicular organoids and germ cell maintenance

In order to explore the effects of specific pro-inflammatory factors (known to be active in the testis *in vivo*) on testicular organoid generation, testicular cells from 20-d*pp* rats were cultured with IL-1α (1 and 10 ng/mL) and TNFα (1 and 10 ng/mL) for 10 days using the 3-LGS. Treatment with IL-1α at both 1 and 10 ng/mL significantly decreased the average area of STSs to 1446.9 and 1567.8 μm^2 respectively, when compared with controls

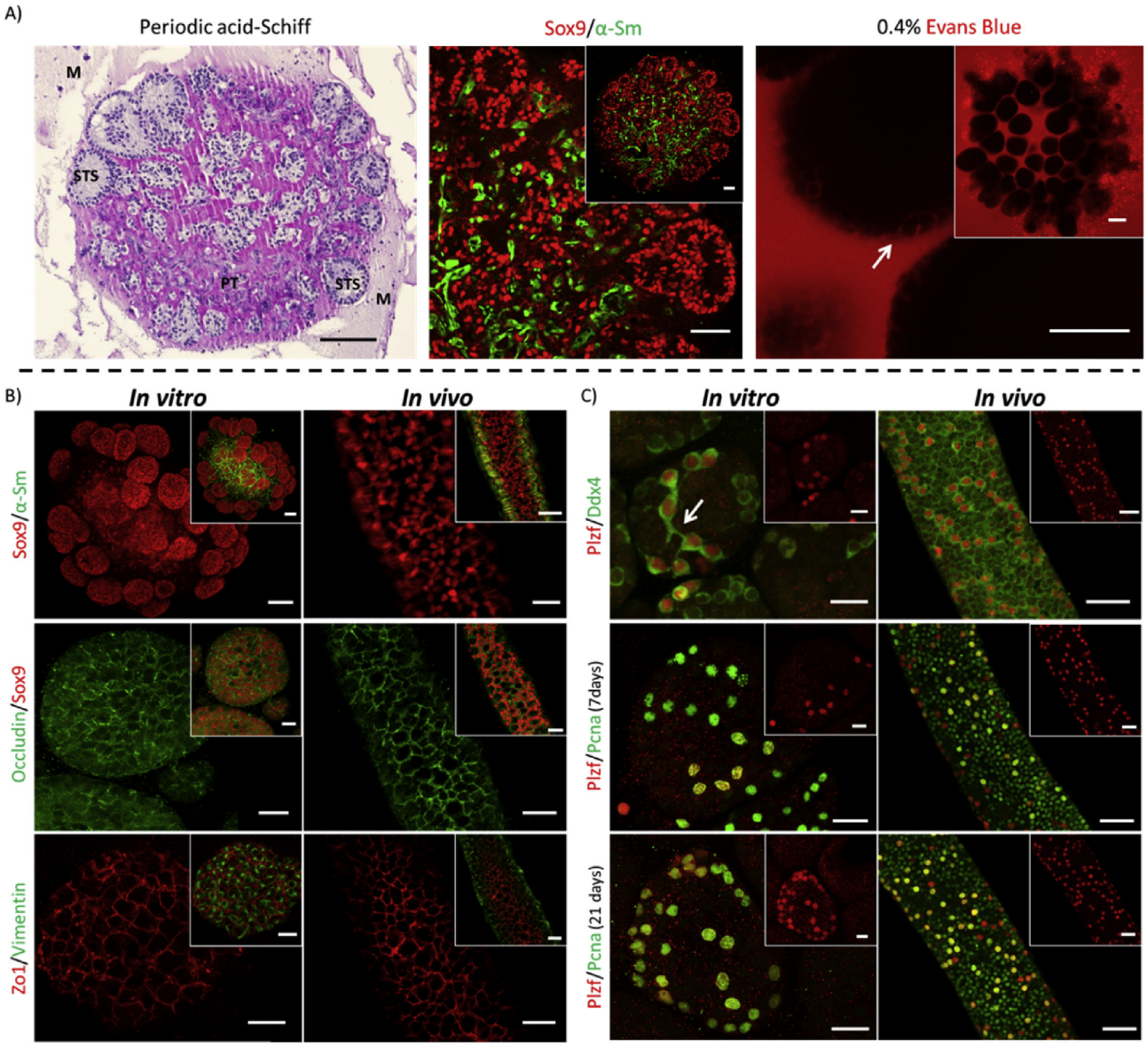

Fig. 3. Rat testicular organoid characterization: BTB formation and germ cell establishment. (A) 20-d*pp* rat cell testicular organoid section stained with periodic acid-Schiff reagent, displaying STS peritubular cells (PT) and Matrigel (M) (scale bar: 100 μm). Testicular organoid transversal section (20-d*pp* rat cells) displaying the disposition of Sertoli (Sox9) and peritubular cells (α-Sm) (scale bar: 50 μm). Testicular organoid impermeability to 0.4% Evans Blue displays evidence of BTB formation *in vitro*. Scale bar: 50 μm (high magnification); 100 μm (low magnification). Evans Blue was observed to infiltrate STSs up to the level of BTB between adjacent Sertoli cells (arrow). (B) Double immunofluorescence staining against Sox9/α-Sm, occluding/Sox9 and Zo1/vimentin in testicular organoid *in vitro* (20-d*pp* rat cells, 7 days in culture) and seminiferous tubules (20-d*pp* rat) showing similarities between *in vitro* and *in vivo* in terms of Sertoli cell and BTB protein component organization. Scale bars: Sox9/α-Sm, 100 μm (*in vitro*), 20 μm (*in vivo* high magnification), 50 μm (*in vivo* low magnification); occludin/Sox9, 20 μm and Zo1/vimentin, 20 μm. (C) Double immunofluorescence staining against Plzf/Ddx4 and Plzf/Pcna showing the cellular chain formation and proliferation capacity of undifferentiated germ cells. The arrow points cytoplasmic bridges between undifferentiated germ cells. Scale bars: 25 μm (*in vitro*), 50 μm (*in vivo*).

(6581.3 μm^2). As regards TNFα treatments, the STSs formed did not show differences in terms of size compared with the controls when a concentration of 1 ng/mL was applied (6450.6 μm^2). However, when TNFα was used at 10 ng/mL, a significant decreasing effect was observed (5186.9 μm^2) (Fig. 5). The bright-field and immunofluorescent images for all conditions are displayed in Suppl. Fig. 6a.

To further display the effects of IL-1α and TNFα on organoid formation, the area occupied by formed STSs in the whole colony (ratio total STS area/total colony area) was determined. Exposure to IL-1α led to a significant decrease in the area occupied by STSs at both 1 (17.1%) and 10 ng/mL (25.4%) when compared with controls (60.4%). On the other hand, treatment with TNFα did not show significant differences in the ratio total STS area/total colony area compared with controls, when doses of 1 (67.6%) and 10 ng/mL (62.1%) were used (Fig. 5).

The influence of IL-1α and TNFα was also investigated in terms of germ cell maintenance by calculation of the ratio germ cells/total cells. IL-1α caused a significant decrease in germ cell maintenance at both 1 (0.2%) and 10 ng/mL (0.2%) when compared with controls (6.3%). Treatment with TNFα showed a direct relationship between drug concentration and germ cell maintenance. At a concentration of 1 ng/mL there was a statistically significant decrease in germ cell maintenance (4.8%), which was also observed at a concentration of 10 ng/mL (2.4%) (Fig. 5).

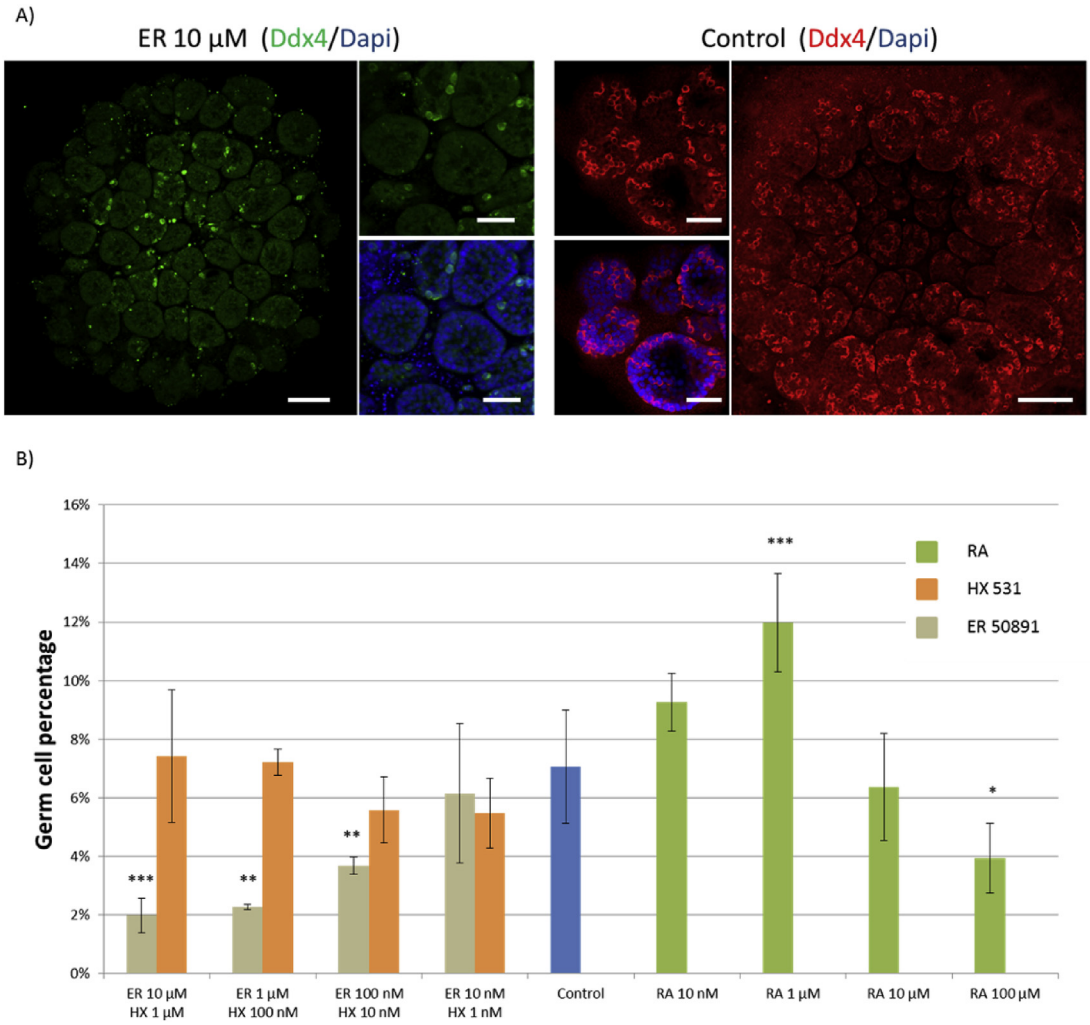

Fig. 4. The role of RA in germ cell maintenance on testicular organoids. (A) Testicular organoids stained for Ddx4 using immunofluorescence after treatment with 10 µM ER 50891, and under control conditions for 10 days. Scale bar: 500 µm (high magnification); 100 µm (low magnification). (B) Effect of RA, ER 50891 and HX 531 on germ cell maintenance compared with control conditions. RA (1 µM) led to an increase in germ cell maintenance, while treatment with ER 50891 (10 µM–100 nM) decreased germ cell maintenance when compared with controls. Statistical methods: One Way ANOVA normality test: Shapiro–Wilk; multiple comparison versus control group: Holm-Sidak; ***P < 0.001; **P < 0.01; *P < 0.05.

Additionally, the presence of Zo-1 and occludin tight junction proteins were sought by immunohistochemistry when testicular cells from 20-d*pp* rats were cultured for 7 days with IL-1α (1 ng/mL) and TNFα (1 ng/mL). Treatment with IL-1α led to the absence of occludin and to an interrupted pattern of Zo-1 distribution when compared with controls, where a well-defined net of both proteins was detected. Regarding the treatment with TNFα, the presence and distribution of both Zo-1 and occludin were not as influenced as with IL-1α, but they were not as homogeneous as observed in the controls (Fig. 6).

3.7. Testicular organoids formed in vitro can be disturbed by treatment with IL-1α and this effect cannot be rescued

To understand whether testicular organoids can be used not only to study the effects of experimental factors on STS formation and germ cell establishment, but also their influences on formed STSs and established germ cells, we allowed the formation of testicular organoids that were then treated with IL-1α.After 7 days of culture under control conditions, IL-1α (1 ng/mL) was added for an additional 7 days (7cont/7 IL-1α). After 14 days, 7cont/7 IL-1α STSs were significantly smaller than those observed in samples cultured in control conditions for 14 days (14cont), with average areas of 3908.6 μm^2 and 13975.1 μm^2 respectively. Moreover, 7cont/7 IL-1α STSs showed an average area even smaller than STSs cultured in control conditions for 7 days (7cont) (6529.6 μm^2). To test if the effect of IL-1α on Sertoli cell organization is reversible, testicular cells from 20-d*pp* rats were exposed to IL-1α for 7 days and then cultured for another 7 days in control conditions (7 IL-1α/7cont). Under these experimental conditions, the average area of STSs was 914.2 μm^2, which is in the same range as STSs formed after 7 days (933.3 μm^2) and 14 days (1079.1 μm^2) under the influence of IL-1α. Additionally, 7 IL-1α/7cont STSs were found to be significantly smaller than 7cont and 14cont STSs, which confirmed the irreversible negative effect of IL-1α in terms of STS generation (Fig. 7). Bright-field and immunofluorescent images for all conditions are displayed in Suppl. Fig. 6b.

The area occupied by the STSs per colony was also determined in these experimental conditions. In a 7cont/7 IL-1α setting, the area occupied by STSs (46.5%) was significantly less than in 7cont (70.5%) and 14cont (82.2%) conditions, but significantly more than in 7 IL-1α (9.5%) and 14 IL-1α (17.7%) conditions. These results

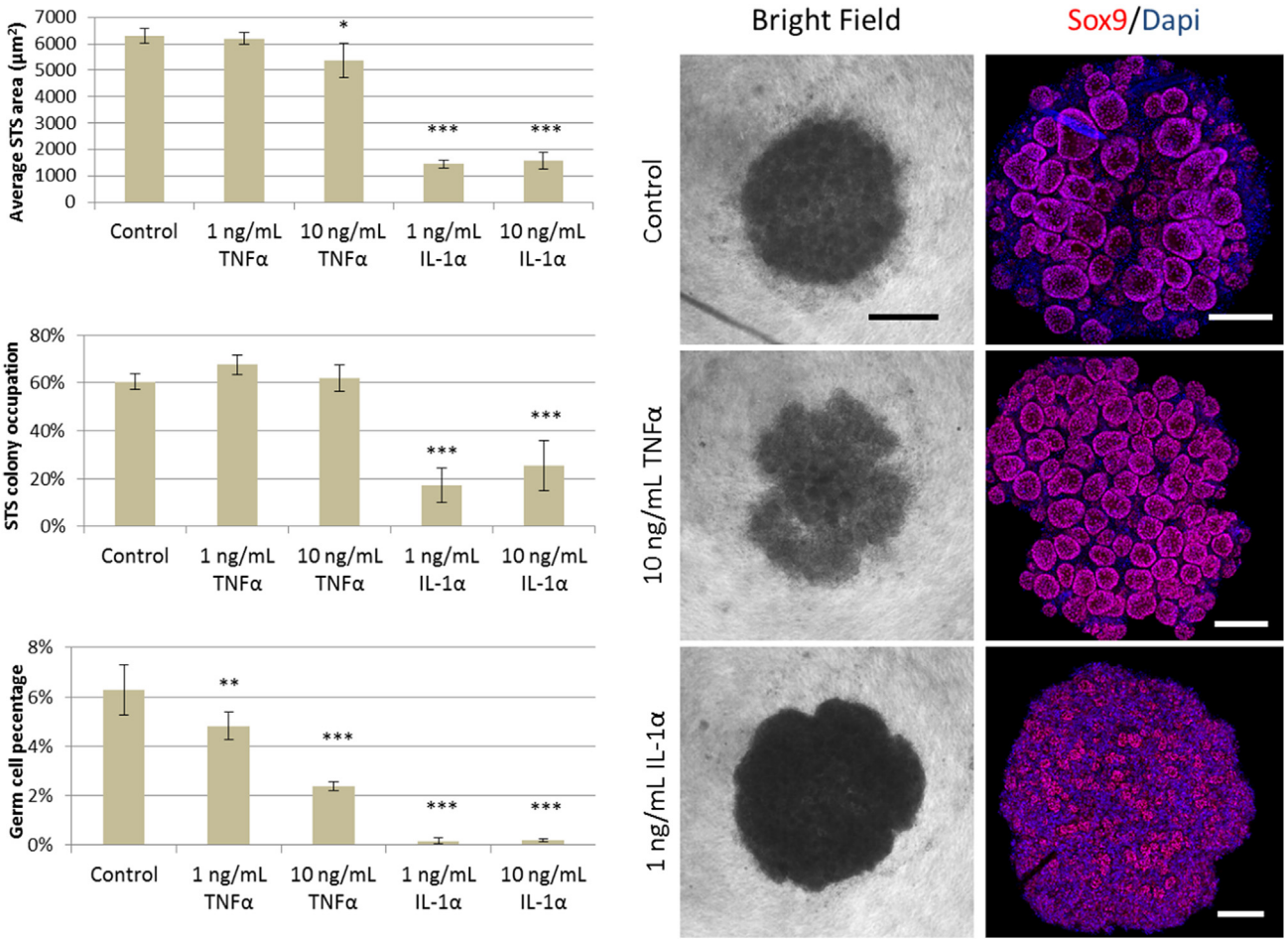

Fig. 5. IL-1α and TNF influence organoid formation and germ cell maintenance. Treatment with IL-1α at both 1 and 10 ng/mL and treatment with TNFα at 10 ng/mL decreased the average area of formed STSs. In addition, fewer STSs were found to occupy the total colony area when testicular cells were allowed to reorganize under the influence of IL-1α at both 1 and 10 ng/mL. Germ cell maintenance decreased when IL-1α and TNFα at both 1 and 10 ng/mL were utilized. Bright-field microscopy and immunofluorescence for Sox9 displayed STS organization on the organoid after 10 days of culture. Scale bar: 500 µm (bright field); 200 µm (immunofluorescence). Statistical methods: One Way RM ANOVA normality test: Shapiro–Wilk; multiple comparison versus control group: Holm-Sidak; ***P < 0.001; **P < 0.01; *P < 0.05.

confirm the previous observation that 7cont/7 IL-1α STSs not only stop growing but also start occupying less area in the whole colony. In the case of 7 IL-1α/7cont conditions, the area occupied by STSs (15.8%) was in the same range as in 7 IL-1α and 14 IL-1α settings, which revealed impaired capacity of Sertoli cells to further form and increase the area occupied by STSs after treatment with IL-1α (Fig. 7).

In addition to the above, germ cell maintenance was also calculated for all experimental conditions. After 7 days of culture in control conditions the ratio germ cell count/total cell count was 12.30%, which decreased significantly to 3.8% when STSs were cultured for an additional 7 days in the same conditions (14cont). In 7 IL-1α and 14 IL-1α conditions, germ cell maintenance also decreased from 7 to 14 days (0.2%–0.04%) and both were significantly lower than in 7cont and 14cont conditions. Regarding 7cont/7 IL-1α and IL-1α7/cont7 conditions the germ cell count/total cell count ratios were 0.2% and 0.02%, being in the same range as in 7 IL-1α and 14 IL-1α conditions, but significantly lower than in 7cont and 14cont setups (Fig. 7).

4. Discussion

In the last years, a promising class of *in vitro* systems, which models organogenesis and/or specific organ functionalities, has resurged [19–21]. An increasing number of studies have described the formation of organ-like structures, named organoids, from pluripotent stem or primary cells [22–24]. Altogether, these findings contributed to the creation of robust and complex *in vitro* models which better mimic *in vivo* conditions and allow researchers to address more challenging scientific questions. In our study, the 3-LGS allows the formation of rat testicular organoids from primary cells, in a robust and efficient way, and offered us a new platform to explore the germ-to-somatic cell associations exclusively *in vitro*.

In the 3-LGS, testicular cells at a concentration of 44 million/mL are suspended in Matrigel and placed between two layers of Matrigel without cells. This technique differs from that which is commonly used in conventional 3D models, where cells are equally distributed in the supportive scaffold [7,11,25]. Thought, our approach is in line with a previous study where lung cells reorganized in branch-like structures when cultured at a high concentration and in a restricted volume (1 µL) surrounded by only Matrigel [26], we here used instead a system of layers that increases the surface area between the layer with and the layers without cells. This approach increased the area where exchange of factors between layers can occur and where cells can become reorganized into STSs (Fig. 8). This system of layers also allows the use of a greater cell suspension volume, consequently generating larger

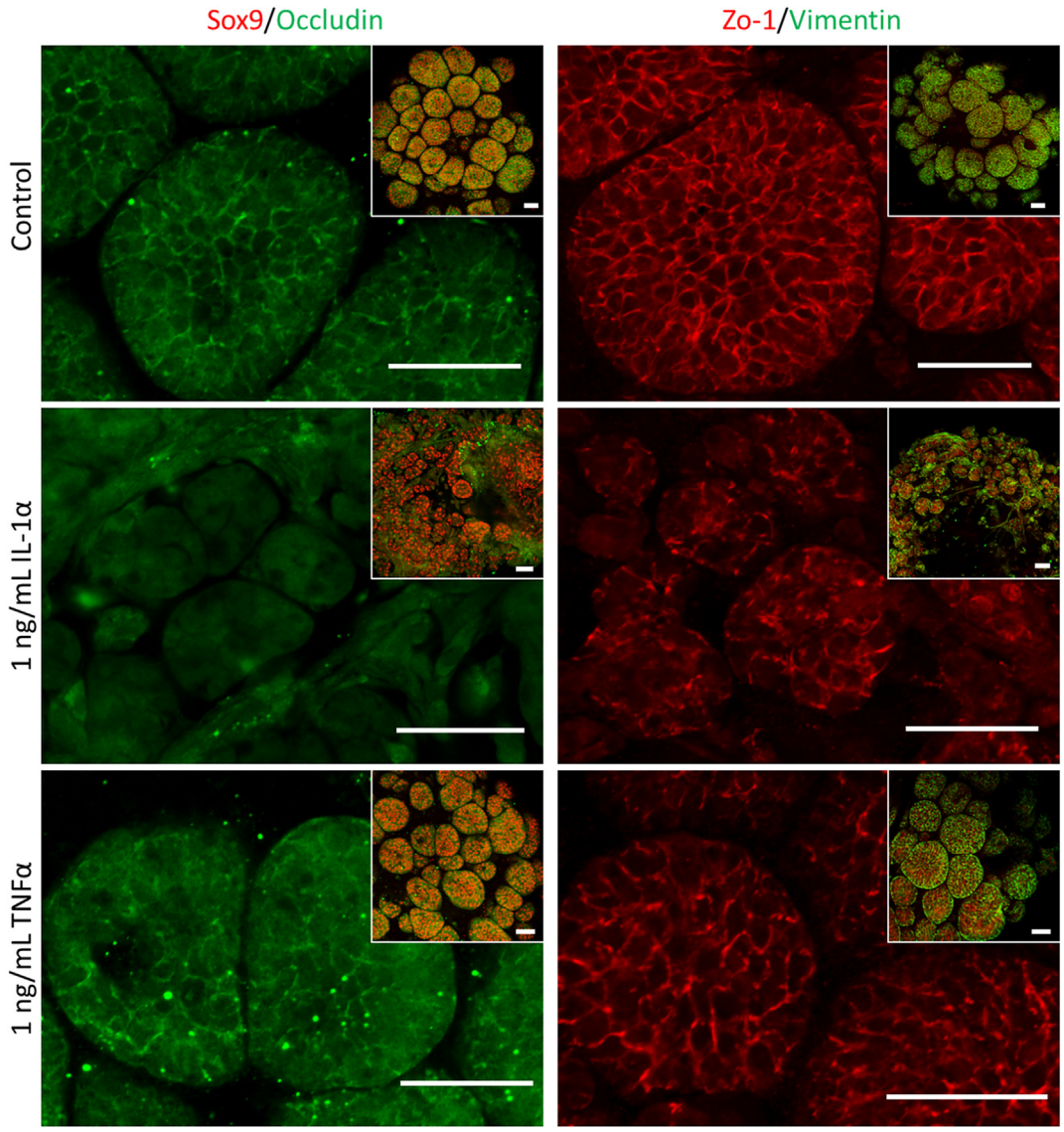

Fig. 6. IL-1α and TNFα influence BTB protein organization. Testicular organoids were treated with IL-1α and TNFα at 1 ng/mL for 7 days. Immunofluorescence staining against BTB proteins Zo1 and occludin showed that treatment with IL-1α resulted in absence of occludin and an interrupted pattern of Zo-1 distribution when compared with control cultures. After treatment with TNFα, the presence of both Zo-1 and occludin was not as greatly disturbed as with IL-1α, but the distribution pattern was not homogeneous as observed in controls. Scale bar: 50 μm.

organoids. In the study by Hagiwara and colleagues, the action of activator factors on neighbouring cells and diffusion of inhibitory factors into the surrounding areas was mentioned as a reason behind cellular reorganization [26]. In addition to Hagiwara's interpretation, we created a hypothetical model to explain the formation of the organoids based on the concepts of molecular diffusion and concentration gradient [27,28]. Under the light of these notions, we think that the formation of organ-like structures in our system is supported by the concentration gradient generated between the layers: cellular metabolites are more concentrated in the layer with cells and consequently they diffuse towards the layers without cells and finally to the medium, while factors present in the Matrigel and culture medium (rapidly consumed by cells) will diffuse from the layers without cells towards the layer with cells (Fig. 8). In the space between layers, the cellular metabolites will then be less concentrated and the factors present in the Matrigel and medium more available than in the centre of the layer with cells. The two concentration gradients (outflow of cellular products and inflow of factors present in the Matrigel and medium) allow the formation of STSs in the area between layers (Fig. 8). Supporting this hypothesis, such STS formation does not occur when the same cellular concentration is applied in a single layer of Matrigel (conventional 3D approach), underlining the importance of the concentration gradient and free space offered by the surrounding layers in the 3-LGS.

The differences detected among the different ages tested in terms of organoid formation and migration profile might be related to the distinct Sertoli cell proportions in the different stages of testicular development, as described for humans [29]. Concerning 60-d*pp* rats, the Sertoli cell proportion is less than in 20-d*pp* rats because the germ cell fraction is increased [29]. This dilution effect, together with the fact that adult Sertoli cells can be impaired at a higher rate than 20-d*pp* rat cells during the digestion process, because of the presence of cytoplasmatic branches between germ cells, may inhibit the formation of STSs. Regarding 5–8-d*pp* rats, the relative number of Sertoli cells is less and the relative number of

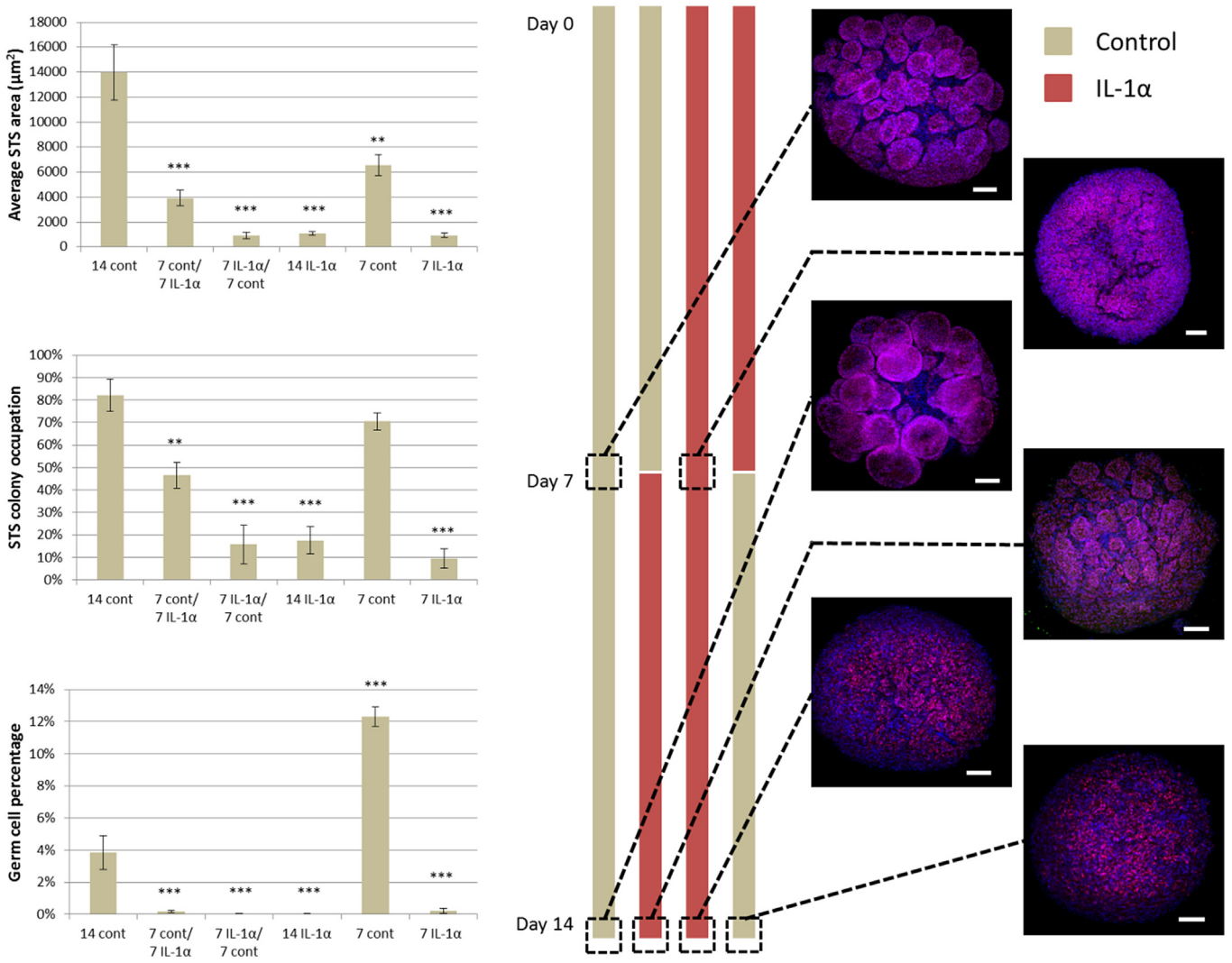

Fig. 7. IL-1α treatment influences STS organization and germ cell maintenance on the organoids. Scheme of the experimental conditions utilized to test the effect of IL-1α at 1 ng/mL on formed organoids. After 7 days of culture in control conditions, IL-1α was added for an additional 7 days. At the end of the experiment, 7cont/7 IL-1α STSs were smaller than those observed in samples cultured in control conditions for 7 and 14 days. Seven days of IL-1α treatment on formed testicular organoids (7cont/7 IL-1α) resulted not only in growth arrest but also in shrunken STSs. Germ cell maintenance was also impaired in 7cont/7 IL-1α conditions compared with 14 cont cultures. Further, the effect of IL-1α on Sertoli cell organization is not reversible, because 7 IL-1α/7cont cultures showed similar STS average areas and germ cell maintenance as both 7 IL-1α and 14 IL-1α control cultures. Immunofluorescence staining against Sox9 (red) shows STS organization at specific time points and particular experimental conditions (DAPI in blue). Scale bar: 100 μm. Statistical methods: One Way RM ANOVA normality test: Shapiro–Wilk; multiple comparison versus control group: Holm-Sidak; ***$P < 0.001$; **$P < 0.01$. (For interpretation of the references to colour in this figure legend, the reader is referred to the web version of this article.)

interstitial cells is greater than in 20-d*pp* rats [29]. However, STSs were observed at low cell concentrations when 5–8-d*pp* rat cells were used, showing that Sertoli cells can still become reorganized, while peritubular cells were detected throughout the colony, forming a net-like structure and involving the STSs. At this early stage, peritubular cells are more immature (e.g. actin filaments are not formed) and more proliferative [30,31], which might explain their faster migration compared with 20-d*pp* rat cells. Moreover, this net-like structure involving small aggregates of Sertoli cells kept the colony more static in terms of migration activity and inhibited the formation of STSs by 5–8-d*pp* rat Sertoli cells.

Backing up the previous models [8,10,32], our system represents an innovative platform to study distinct aspects of the SSC niche *in vitro*. The organoids generated by the 3-LGS showed similarities with the germ and Sertoli cell organization observed *in vivo*: Sertoli cells organized themselves into STSs and displayed epithelium formation within 7 days of culture. On the other hand, peritubular cells did not completely reorganize themselves around the STSs in the same fashion as they surround the seminiferous tubules *in vivo*, which might be related to the mesenchymal cell features of these cells [33].

Nevertheless, STSs displayed to be impermeable to Evans Blue, a small molecule used to test BTB integrity *in vivo* [34], and to express occludin and Zo-1 proteins, known to be components of tight junctions and therefore BTB constituents, between Sertoli cells. Altogether, these results indicate the presence of a functional BTB in the generated organoids. Furthermore, germ cells organized on the STSs in a comparable manner as observed *in vivo*, where undifferentiated germ cells are located between the basal membrane and the BTB forming colonies in the shape of cellular chains [35]. In our study, cellular chains of undifferentiated germ cells were also detected on STSs. Although germ cell counts decreased over the time in culture, we also demonstrated that, after 21 days in culture, the remaining undifferentiated germ cells are still proliferating

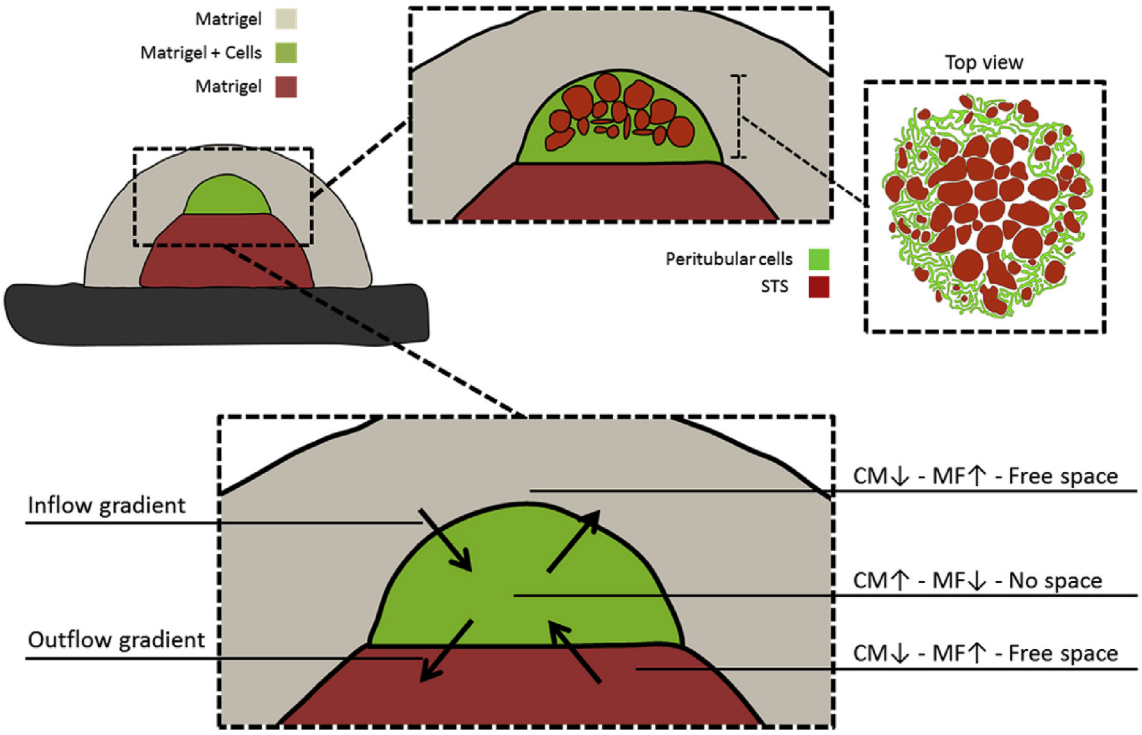

Fig. 8. Schematic representation of testicular organoid generation via the 3-LGS. Testicular cells combined with Matrigel at a final concentration of 44 million cells/mL were placed between two layers of Matrigel without cells and were found to reorganize themselves into seminiferous-like structures. The layer approach allows cellular compartmentalization in a 3D system and at the same time permits exchange of factors between layers with and without cells. Organoid formation in the 3-LGS can be mainly explained by the gradients generated between the layers. The first gradient is produced by cellular metabolites (CM) generated in the layer with cells and which diffuse to the layers without cells. The second gradient is created by factors present in the Matrigel and culture medium (MF), which are rapidly consumed by cells and which diffuse from the layers without cells towards the middle layer. In the space between layers, CM will become less concentrated and MF more concentrated than in the centre of the layer with cells. Both gradients (outflow of CM and inflow of MF) support the formation of STSs in the area between layers. A schematic top view of a testicular organoid is also displayed in the picture.

suggesting that improved culture conditions, by adding or inhibiting factors of interest, might contribute to maintain these cells for longer periods in culture and to help in the search for new factors involved in germ cell proliferation.

RA is one of the essential factors for germ cell differentiation and maintenance. It has been shown that vitamin A-deficient rats display impaired spermatogenesis and a decrease in germ cell counts, which can be recovered by RA administration [36]. Our results show that medium components with RA-like effect are not enough to promote the maximum degree of germ cell maintenance, as supplementation with extra RA (1 μM) increased germ cell numbers. On the other hand, the inhibitory effect of ER 50891 led to a decrease in germ cell maintenance when 100 nM–10 μM supplementations were utilized. This decrease in germ cell numbers was not observed when doses of ER 50891 are enough to inhibit RARα (IC_{50} = 31.2 nM), but instead, decreases were detected at doses known to inhibit RARγ and RARβ (IC_{50} = 432 and 535 nM respectively). These results are in line with those of previous studies which show that RAR subtype γ is the one responsible for RA pathway activation in germ cells [37,38]. Moreover, RA inhibition with ER 50891 leads to decreased germ cell maintenance that reaches a plateau at higher concentrations, suggesting the existence of a germ cell population unresponsive to RA, as also suggested by Ikami and colleagues [38]. In contrast, germ cell numbers did not vary significantly when HX 531 was applied, suggesting a non-essential role of RXR in germ cell maintenance, as also reported *in vivo* [39,40].

Both IL-1α and TNFα are pro-inflammatory cytokines involved in BTB regulation and are suggested to act locally to momentarily disrupt the tight junctions present in this barrier, allowing germ cells to pass through and further differentiate inside the lumen of the seminiferous tubules [41]. Our results are in concordance with those of previous studies where IL-1α and TNFα have been shown to disturb the BTB in adult rats and decrease germ cell counts *in vivo* [42]. The impairment of BTB formation in STSs by treatment with IL-1α and TNFα can explain the decrease in STS average area. When immature Sertoli cells were cultured on a petri dish under the influence of IL-1α, they became more motile and proliferative, as demonstrated in an *in vitro* study with 8–9 *dpp* rat Sertoli cells [43]. Moreover, no occludin and an interrupted pattern of Zo-1 were detected in testicular organoids formed in the presence of IL-1α, showing evidence of BTB impairment. The insufficient Sertoli cell-to-cell connections can also explain the decreased number of Sertoli cells that contribute to STS formation in cultures treated with IL-1α. Altogether, our results demonstrate that damage of Sertoli cell organization by IL-1α is accompanied by decreasing germ cell maintenance, providing evidence that the testicular organoid microenvironment is essential for germ cell establishment *in vitro* [44]. Finally, we also demonstrated that the effect of IL-1α on formed organoids is irreversible, because 7 IL-1α/7cont STSs showed similar average areas as both 7 IL-1α and 14 IL-1α STSs. The irreversible effect of IL-1α in BTB disorganization and germ cell loss has also been demonstrated *in vivo* [42].

In summary, the 3-LGS supports the generation of rat testicular organoids, representing a novel approach to reassemble seminiferous-like structures *in vitro*. Moreover, our model permitted us to verify the role of RA and the pro-inflammatory cytokines IL-1α and TNFα in BTB formation and germ cell maintenance. The similarities of our results to those of previous *in vivo* studies validated the use of testicular organoids to explore distinct

aspects of testicular biology and SSC niche *in vitro* (overview at Fig. 1). Although advanced steps of spermatogenesis were not detected using the basic conditions in this study, the future utilization of still unknown factors involved germ cell differentiation might improve spermatogenesis efficiency in this model. The fact that the starting point is a single cell suspension will bring the opportunity to genetically modify, include or exclude (by sorting) a cell population of interest. This previous manipulation of cells that will constitute the organoids might allow us to engineer experimental conditions to seek for essential factors and somatic cells involved in the regulation of the SSC niche and in testicular development. Moreover, we propose that the 3-LGS can be used to allow the organization of SSCs and testicular somatic cells differentiated from pluripotent stem cells into testicular organoids and to improve or support the formation of organ-like structures in other tissue-engineering contexts.

Funding information

This work was supported by the HKH Kronprinsessan Lovisas förening för barnasjukvård, Frimurare Barnhuset in Stockholm; the Paediatric Research Foundation, Jeanssons Foundation (JS2014-0091); Sällskåpet Barnåvard in Stockholm; Swedish Research Council/Academy of Finland (2012-6352); Emil and Wera Cornells Foundation; Samariten Foundation; the Swedish Childhood Cancer Foundation (PR2016-0124, TJ2016-0093); the EU-FP7-PEOPLE-2013-ITN (603568) “Growsperm”.

Conflicts of interest

None.

Author contributions

J.P.A.L., and J.-B.S. designed the study. J.P.A.L. performed the experiments, and the analyses of data. J.P.A.L., J.-B.S. and OS interpreted the data. O.S., and J.-B.S. obtained funding. J.P.A.L. wrote the manuscript and all authors contributed to critical review and approve the final version of the manuscript.

Acknowledgements

We thank Ahmed Osman for support with confocal microscopy and technical advice and Luís Lopes for assistance with graphic design of the pictures in this manuscript. We are grateful to Liang Zhang, Jacopo Fontana and Irja Eggertsen for technical support in the animal facilities as well as to Elisabeth Villow for technical assistance in sectioning.

Appendix A. Supplementary data

Supplementary data related to this article can be found at http://dx.doi.org/10.1016/j.biomaterials.2017.03.025.

References

[1] R.A. Hess, L.R. Franca, Spermatogenesis and cycle of the seminiferous epithelium, in: C.Y. Cheng (Ed.), Molecular Mechanisms in Spermatogenesis, Springer, New York, NY, 2008, pp. 1–15.
[2] B.P. Setchell, Blood-testis barrier, junctional and transport proteins and spermatogenesis, in: C.Y. Cheng (Ed.), Molecular Mechanisms in Spermatogenesis, Springer, New York, NY, 2008, pp. 212–233.
[3] G.F. Weinbauer, C.M. Luetjens, M. Simoni, E. Nieschlag, Physiology of testicular function, in: E. Nieschlag, H.M. Behre, S. Nieschlag (Eds.), Andrology: Male Reproductive Health and Dysfunction, Springer, Berlin, Heidelberg, 2010, pp. 11–59.
[4] M. Nagano, B.-Y. Ryu, C.J. Brinster, M.R. Avarbock, R.L. Brinster, Maintenance of mouse male germ line stem cells in vitro, Biol. Reprod. 68 (2003) 2207–2214.
[5] M. Sousa, N. Cremades, C. Alves, J. Silva, A. Barros, Developmental potential of human spermatogenic cells co-cultured with Sertoli cells, Hum. Reprod. 17 (2002) 161–172.
[6] C.A. Staub, Century of Research on mammalian male germ cell meiotic differentiation in vitro, J. Androl. 22 (2001) 911–926.
[7] A. Reda, M. Hou, L. Landreh, K.R. Kjartansdóttir, K. Svechnikov, O. Söder, et al., In vitro spermatogenesis – optimal culture conditions for testicular cell survival, germ cell differentiation, and steroidogenesis in rats, Front. Endocrinol. 5 (2014) 21.
[8] K. Gassei, S. Schlatt, J. Ehmcke, De novo morphogenesis of seminiferous tubules from dissociated immature rat testicular cells in xenografts, J. Androl. 27 (2006) 611–618.
[9] A. Honaramooz, S.O. Megee, R. Rathi, I. Dobrinski, Building a testis: formation of functional testis tissue after transplantation of isolated porcine (Sus scrofa) testis cells, Biol. Reprod. 76 (2007) 43–47.
[10] T. Yokonishi, T. Sato, K. Katagiri, M. Komeya, Y. Kubota, T. Ogawa, In vitro reconstruction of mouse seminiferous tubules supporting germ cell differentiation, Biol. Reprod. 89 (15) (2013) 1–6.
[11] J.-B. Stukenborg, S. Schlatt, M. Simoni, C.-H. Yeung, M.A. Elhija, C.M. Luetjens, et al., New horizons for in vitro spermatogenesis? An update on novel three-dimensional culture systems as tools for meiotic and post-meiotic differentiation of testicular germ cells, Mol. Hum. Reprod. 15 (2009) 521–529.
[12] J.-B. Stukenborg, J. Wistuba, C.M. Luetjens, M.A. Elhija, M. Huleihel, E. Lunenfeld, et al., Coculture of spermatogonia with somatic cells in a novel three-dimensional soft-agar-culture-system, J. Androl. 29 (2008) 312–329.
[13] M. Abu Elhija, E. Lunenfeld, S. Schlatt, M. Huleihel, Differentiation of murine male germ cells to spermatozoa in a soft agar culture system, Asian J. Androl. 14 (2012) 285–293.
[14] T. Sato, K. Katagiri, Y. Kubota, T. Ogawa, In vitro sperm production from mouse spermatogonial stem cell lines using an organ culture method, Nat. Protoc. 8 (2013) 2098–2104.
[15] A. Reda, M. Hou, T.R. Winton, R.E. Chapin, O. Söder, J.-B. Stukenborg, In vitro differentiation of rat spermatogonia into round spermatids in tissue culture, Mol. Hum. Reprod. 22 (2016) 601–612.
[16] L. Dumont, B. Arkoun, F. Jumeau, J.P. Milazzo, A. Bironneau, D. Liot, et al., Assessment of the optimal vitrification protocol for pre-pubertal mice testes leading to successful in vitro production of flagellated spermatozoa, Andrology 3 (2015) 611–625.
[17] A. Steinberger, E. Steinberger, W.H. Perloff, Mammalian testes in organ culture, Exp. Cell Res. 36 (1964) 19–27.
[18] T. Sato, K. Katagiri, A. Gohbara, K. Inoue, N. Ogonuki, A. Ogura, et al., In vitro production of functional sperm in cultured neonatal mouse testes, Nature 471 (2011) 504–507.
[19] H. Clevers, Modeling development and disease with organoids, Cell. 165 (2016) 1586–1597.
[20] H. Hisha, T. Tanaka, S. Kanno, Y. Tokuyama, Y. Komai, S. Ohe, et al., Establishment of a novel lingual organoid culture system: generation of organoids having mature keratinized epithelium from adult epithelial stem cells, Sci. Rep. 3 (2013) 3224.
[21] J.P. Morgan, P.F. Delnero, Y. Zheng, S.S. Verbridge, J. Chen, M. Craven, et al., Formation of microvascular networks in vitro, Nat. Protoc. 8 (2013) 1820–1836.
[22] C. Willyard, The boom in mini stomachs, brains, breasts, kidneys and more, Nature 523 (2015) 520–522.
[23] M.A. Lancaster, M. Renner, C.-A. Martin, D. Wenzel, L.S. Bicknell, M.E. Hurles, et al., Cerebral organoids model human brain development and microcephaly, Nature 501 (2013) 373–379.
[24] T. Takebe, K. Sekine, M. Enomura, H. Koike, M. Kimura, T. Ogaeri, et al., Vascularized and functional human liver from an iPSC-derived organ bud transplant, Nature 499 (2013) 481–484.
[25] K. Gassei, J. Ehmcke, M.A. Wood, W.H. Walker, S. Schlatt, Immature rat seminiferous tubules reconstructed in vitro express markers of Sertoli cell maturation after xenografting into nude mouse hosts, Mol. Hum. Reprod. 16 (2010) 97–110.
[26] M. Hagiwara, F. Peng, C.-M. Ho, In vitro reconstruction of branched tubular structures from lung epithelial cells in high cell concentration gradient environment, Sci. Rep. (2015) 5.
[27] R. Hine, E. Martin, Concentration Gradient. A Dictionary of Biology. Oxford Reference, Oxford University Press, 2016.
[28] R. Hine, E. Martin, Diffusion. A Dictionary of Biology. Oxford Reference, Oxford University Press, 2016.
[29] R. Rey, Regulation of spermatogenesis, in: O. Söder (Ed.), The Developing Testis Physiology and Pathophysiology, Endocrine Development, Basel, 2003, pp. 38–55.
[30] L.D. Russell, A. Bartke, J.C. Goh, Postnatal-development of the sertoli-cell barrier, tubular lumen, and cytoskeleton of Sertoli and myoid cells in the rat, and their relationship to tubular fluid secretion and flow, Am. J. Anat. 184 (1989) 179–189.
[31] F. Palombi, D. Farini, M. Salanova, S. Degrossi, M. Stefanini, Development and cytodifferentiation of peritubular myoid cells in the rat testis, Anat. Rec. 233 (1992) 32–40.
[32] J.H. Lee, H.J. Kim, H. Kim, S.J. Lee, M.C. Gye, In vitro spermatogenesis by three-dimensional culture of rat testicular cells in collagen gel matrix, Biomaterials 27 (2006) 2845–2853.

[33] E.R. Shamir, A.J. Ewald, Three-dimensional organotypic culture: experimental models of mammalian biology and disease, Nat. Rev. Mol. cell Biol. 15 (2014) 647–664.
[34] M. Al-Asmakh, J.-B. Stukenborg, A. Reda, F. Anuar, M.-L. Strand, L. Hedin, et al., The gut microbiota and developmental programming of the testis in mice, PloS one 9 (2014) e103809.
[35] B.T. Phillips, K. Gassei, K.E. Orwig, Spermatogonial stem cell regulation and spermatogenesis, Philos. Trans. R. Soc. Lond. B Biol. Sci. 365 (2010) 1663–1678.
[36] A.M.M.V. Pelt, D.G.D. Rooij, Retinoic acid is able to reinitiate spermatogenesis in vitamin a-deficient rats and high replicate doses support the full development of spermatogenic cells, Endocrinology 128 (1991) 697–704.
[37] A. Gely-Pernot, M. Raverdeau, C. Célébi, C. Dennefeld, B. Feret, M. Klopfenstein, et al., Spermatogonia differentiation requires retinoic acid receptor γ, Endocrinology 153 (2012) 438–449.
[38] K. Ikami, M. Tokue, R. Sugimoto, C. Noda, S. Kobayashi, K. Hara, et al., Hierarchical differentiation competence in response to retinoic acid ensures stem cell maintenance during mouse spermatogenesis, Development 142 (2015) 1582–1592.
[39] C. Hogarth, 9-Retinoic acid metabolism, signaling, and function in the adult testis A2-Griswold, in: D. Michael (Ed.), Sertoli Cell Biology, second ed., Academic Press, Oxford, 2015, pp. 247–272.
[40] W. Krezel, V. Dupé, M. Mark, A. Dierich, P. Kastner, P. Chambon, RXR gamma null mice are apparently normal and compound RXR alpha +/-/RXR beta -/-/RXR gamma -/- mutant mice are viable, Proc. Natl. Acad. Sci. U. S. A. 93 (1996) 9010–9014.
[41] H.H.N. Yan, D.D. Mruk, W.M. Lee, C.Y. Cheng, Blood-testis barrier dynamics are regulated by testosterone and cytokines via their differential effects on the kinetics of protein endocytosis and recycling in Sertoli cells, FASEB J. 22 (2008) 1945–1959.
[42] O. Sarkar, P.P. Mathur, C.Y. Cheng, D.D. Mruk, Interleukin 1 alpha (IL1A) is a novel regulator of the blood-testis barrier in the rat, Biol. Reprod. 78 (2008) 445–454.
[43] C. Petersen, C. Boitani, B. Fröysa, O. Söder, Interleukin-1 is a potent growth factor for immature rat Sertoli cells, Mol. Cell. Endocrinol. 186 (2002) 37–47.
[44] C.Y. Cheng, D.D. Mruk, The blood-testis barrier and its implications for male contraception, Pharmacol. Rev. 64 (2012) 16–64.